^{123}I-Labeled Chitinase as Specific Radioligand for In Vivo Detection of Fungal Infections in Mice

Rien Siaens, MSc[1]; Vincent G.H. Eijsink, PhD[2]; Rudi Dierckx, MD[3]; and Guido Slegers, PhD[1]

[1]*Laboratory of Radiopharmacy, Gent University, Gent, Belgium;* [2]*Department of Chemistry and Biotechnology, Agricultural University of Norway, Ås, Norway; and* [3]*Department of Nuclear Medicine, Gent University Hospital, Gent, Belgium*

Given the scarcity of diagnostic tools for invasive fungal infections, the aim of this project was to develop new, specific radiopharmaceuticals for diagnosis of fungal infections. Chitin, which is expressed in the fungal cell wall but is absent in mammalian and bacterial cells, represents a potentially selective target for development of tracers for fungal infections. ChiB_E144Q (ChiB = chitinase B) from *Serratia marcescens* was labeled with ^{123}I, and in vitro and in vivo studies were assessed. **Methods:** ^{123}I labeling of ChiB_E144Q from *S. marcescens* by direct iodination was characterized by high-pressure liquid chromatography (HPLC), and stability was evaluated. The in vitro binding properties of the compound to living bacteria, *Candida albicans*, and *Aspergillus fumigatus* were examined. Scintigraphy was performed and in vivo characteristics were studied in mice with infected thigh muscles. **Results:** An average radiochemical yield of 35% was obtained. Radiochemical purity was >97% with a stability of >24 h as determined by HPLC and instant thin-layer chromatography. The average specific activity of the noncarrier-free ^{123}I-chitinase was 9.25 MBq/μg of enzyme. Binding assays showed virtually no binding to *Eschericha coli* and *Staphylococcus aureus*, and 2.4×10^3 Bq per 1×10^7 cells for *A. fumigatus* and 3.0×10^3 Bq per 1×10^7 cells for *C. albicans* ($P < 0.05$). Binding of the tracer dropped to almost zero for organisms previously incubated with a 50-fold excess of unlabeled enzyme. At 24 h after injection, target-to-nontarget (T/NT) ratios in mice were 20.6 ± 3.6 for *C. albicans* and 15.2 ± 3.7 for *A. fumigatus* infections, respectively, whereas T/NT ratios for *S. aureus* – and *E. coli*–infected thigh muscles or thigh muscles with a sterile inflammation did not exceed 4.9 ± 2.6, 3.0 ± 2.3, and 5.3 ± 2.8, respectively ($P < 0.05$). Target-to-blood ratios for fungus-infected thighs were always >1. **Conclusion:** Our results show that ^{123}I-ChiB_E144Q has affinity in vitro for fungi. In vivo, the tracer accumulates in tissue infected with *C. albicans* and *A. fumigatus* but not in tissue infected with gram-positive or gram-negative bacteria, or in sterile inflammations, proving it to be a valuable SPECT diagnostic.

Key Words: infection imaging; ^{123}I-chitinase; *Candida albicans*; *Aspergillus fumigatus*; bacteria

J Nucl Med 2004; 45:1209–1216

Received Sep. 26, 2003; revision accepted Jan. 14, 2004.

For correspondence or reprints contact: Rien Siaens, MSc, Harelbekestraat 72, 9000 Ghent, Belgium.

E-mail: Rien.Siaens@ugent.be

Specific scintigraphic detection of infection or inflammation remains a challenging issue in the field of nuclear medicine. Being able to distinguish infection from sterile inflammation with radiopharmaceuticals is of clinical importance for the treatment of patients with presumed or established inflammatory disorders (*1*). Given the differences in treatment of fungal infections versus bacterial infections, the distinction between fungal infection, bacterial infection, and sterile inflammation might be valuable for diagnosis of infected patients (*2*).

Due to a significant rise in the number of immunocompromised hosts—due to AIDS, aggressive anticancer therapy, the increase in organ transplants, and so forth—the number of important life-threatening invasive fungal infections, such as invasive aspergillosis and candidiasis has equally increased, despite the significant advances in antifungal therapy (*3,4*). Unfortunately, today, only few diagnostic tools for specific detection of fungal infection are available.

Direct examination and cultivation of any suspicious site of infection are still the main tools of conventional diagnosis but these methods are not very sensitive and often results are obtained too late to be clinically useful (*2,5*). Moreover, laboratory diagnosis of invasive mycoses poses several other problems. In immunocompromised hosts, inflammatory parameters obtained from blood samples are not necessarily abnormal. Sampling often requires invasive procedures that may be risky (*4*). Diagnostic sensitivity of conventional radiologic techniques such as chest radiography, abdominal ultrasound, or CT is dependent on the production of inflammatory tissue, which may not be present, or barely present, in patients with a blunted inflammatory response. These conventional radiologic techniques thus lack sensitivity as well as specificity (*2*).

In the field of radiopharmacy some new types of tracers have been developed for diagnosing fungal infections, such as radiolabeled azoles, radiolabeled EB-A2 monoclonal antibody against *Aspergillus galactomannan*, and ^{99m}Tc-labeled poly(ethyleneglycol) (PEG)–liposomes (*6–8*). The latter method lacks the ability to distinguish between fungal and bacterial infection. However, no microorganism-specific technique has made its way into clinical routine to date

(*9*). Given the scarcity of available diagnostics tools and their lack of specificity or sensitivity, there is an urgent need for new, fast, and accurate diagnostic tools, preferably with affinity toward a wide range of fungi and yeasts (*2*).

The search for novel antifungal drugs exploits the differences between fungi and other species to develop specific accurate therapies that are harmless to the host. The cell wall of fungi and yeasts represents several unique targets for therapy and diagnosing, such as glucans, mannoproteins, and chitin. Since chitin is not present in mammalian or bacterial cells, it represents a highly selective target for chitin-recognizing proteins such as chitinases (*10*). Chitinases cleave the β 1–4 linkage between the *N*-acetylglucosamine residues of chitin and belong to families 18 and 19 of the glycosyl hydrolases. They are found in plants, animals, fungi, bacteria, and even humans, with a wide range of molecular sizes (30–120 kDa) (*11–13*).

Many chitinases possess one or more chitin-binding domains in addition to their catalytic domain, which enable the enzyme to bind intimately to chitin (*14*). Therefore, these enzymes seemed to be an interesting experimental starting point for the development of a specific tracer for a wide range of invasive fungal infections. The possible advantages of radiolabeled chitinases may include that they are not restricted to a certain spectrum of fungi or yeasts, as long as chitin is abundant in their cell wall, and they are not affected by resistant strains in contradiction to most commonly used antifungal drugs and their labeled variants.

The chitinase of our choice was a variant of chitinase B (ChiB) derived from the bacterium *Serratia marcescens*. This is a well-studied enzyme that consists of a catalytic domain and 1 chitin-binding domain (*15,16*). We used a variant of ChiB in which the catalytic acid, Glu-144, has been replaced by glutamine (E144Q). ChiB_E144Q is 4,000-fold less active than the wild-type enzyme, but it retains its chitin-binding domain and it displays wild-type–like binding affinities for chitin-like substrates (*15,16*).

The binding constant for binding of ChiB or ChiB_E144Q to chitin is not known, but preliminary results for ChiB_E144Q as well as studies on similar chitinases (*17–19*) indicate that such constants lie in the low and submicromolar range. It has been shown that the E144Q mutation does not affect binding (*16*). Thus, binding of ChiB_E144Q to chitin is expected to be quite strong.

This article reports on the preparation and characterization of ^{123}I-labeled ChiB_E144Q, a new experimental specific radiopharmaceutical for diagnosis of fungal infections. In vitro binding studies were assessed with different fungi and bacteria. Furthermore, in vivo studies in mice with fungal or bacterial infection were performed. Scintigraphic imaging and postmortem tissue counting provided biodistribution data of the tracer. ^{123}I-Labeled bovine serum albumin was used as a nonspecific control to verify nonspecific uptake in the infected lesions.

MATERIALS AND METHODS

Reagents

ChiB_E144Q was produced and purified in volatile ammonium bicarbonate buffers, as described previously (*20*). The purified enzyme was freeze-dried and redissolved at 1 mg/mL in Tris buffer (20 mmol/L, pH 8). Aliquots of 25 μL were stored at −20°C.

Radiolabeling

Direct iodination was performed according to the commonly used IODO-GEN (Pierce) procedure. Aliquots were thawed and transferred to precoated IODO-GEN vials. For binding studies and biodistribution studies, 1–3 μL of 37 MBq ^{123}I (Nycomed Amersham) in 0.05 mol/L NaOH were added to 25 μg thawed ChiB_E144Q and, subsequently, the mixture was incubated at room temperature for 20 min. For scintigraphic studies, 17–25 μL of 370 MBq ^{123}I in 0.05 mol/L NaOH were added to 50 μg of thawed ChiB_E144Q and incubated at room temperature for 20 min. The labeled enzyme was applied to a Sephadex G25 (PD10; Pharmacia) column for purification and eluted with 0.5% bovine serum albumin (BSA) in phosphate-buffered saline (PBS) (pH 8.0). The purified tracer solution was used as such. A series of syntheses was prepared with different reaction times (5–30 min) ($n = 1$). The radiochemical purity of the tracer was determined by size-exclusion high-pressure liquid chromatography (HPLC) using 0.1 mol/L KH_2PO_4 buffer (pH 8.1) as the liquid phase (0.8 mL/min) on an Ultrahydrogel column (7.8 × 300 mm; Waters) connected to a UV-VIS spectrophotometer (280 nm) (SPD-6AV; Shimadzu) and a NaI γ-counter (model 2200; Ludlum).

In addition, the tracer was monitored during 30 h in PBS (pH 8) supplemented with 0.5% BSA and in murine serum to determine its stability by instant thin-layer chromatography (ITLC) on silica gel–impregnated ITLC strips (1 × 10 cm; Gelman Laboratories) using 0.1 mol/L citrate (pH 6.5) as the mobile phase. As a nonspecific control, BSA was labeled in an identical way using equimolar amounts of peptide and radioisotope. ^{67}Ga-Citrate (Mallinckrodt) was used as a positive control.

Microorganisms

Staphylococcus aureus 6538 (*S. aureus*), *Escherichia coli* 8739 (*E. coli*), *Candida albicans* 10231 (*C. albicans*), and *Aspergillus fumigatus* 1022 (*A. fumigatus*) were obtained from the American Type Culture Collection. Overnight cultures of bacteria were prepared on tryptone soja agar (Oxoid) plates at 37°C. Yeasts and fungi were cultured on sabouraud dextrose agar (Oxoid) during 3–5 d at 22°C. Aliquots of suspensions of harvested microorganisms containing 2×10^8 colony-forming units (cfu) were kept in 1 mL of buffered peptone water (Oxoid) at 4°C for a maximum of 2 wk.

In Vitro Cell-Binding Studies

Small increasing amounts of ^{123}I-ChiB_E144Q were added to 1 mL of incubation buffer (7.52 g/L K_2HPO_4, 1.32 g/L $NaH_2PO_4 \cdot H_2O$, 7.2 g/L NaCl + 0.5% BSA, pH 7.8) containing 1×10^7 cfu of *C. albicans*, 1×10^8 cfu of *A. fumigatus*, and 1×10^7 cfu of *E. coli* or *S. aureus*. Analogous incubations were performed in the presence of a 50-fold excess of unlabeled ChiB_E144Q (1.5×10^{-2} μg/10 μL per tube) to determine the nonspecific binding. (All binding assays or incubations were performed 3 times unless indicated otherwise.) After overnight incubation at 4°C, the cells were centrifuged at 3,500*g* for 6 min, the

supernatant was removed, and the pellet was washed once with 1 mL of the binding buffer. The pellets were counted on a multichannel NaI γ-counter (Cobra Packard). The binding of the tracer to the various organisms is expressed as counts per minute (cpm) of ^{123}I activity bound to 1×10^7 cells after 1 washing-step, corrected for nonspecific binding.

Binding to Mammalian Cells

Binding to mammalian cells was investigated in vivo and assessed as follows. Blood obtained from *nu/nu* mice previously injected with 37–54 kBq ^{123}I-ChiB_E144Q was collected in ethylenediaminetetraacetic acid–coated tubes. The total volume was weighed and counted for its activity. Subsequently, the blood was allowed to sediment for 1 h. The leukocyte-rich plasma was removed and centrifuged for 15 min at 500*g*. The pellet was separated from the supernatant. Finally, 50 μL of trichloroacetic acid were added to the supernatant to coagulate the proteins. Erythrocytes, leukocytes, and protein fraction were washed with 1 mL of PBS. As the control, the distribution at 24 h after injection of 37–54 kBq ^{123}I between the different blood fractions was determined. The results are expressed as % activity/% (g) blood.

Thigh Muscle Infections

Swiss *nu/nu* mice and NMRI mice of random sex (body weight, 20–25 g) were obtained from an in-house breeding program. All animal studies were performed in compliance with the local Experimental Animal Ethical Committee and the Belgian laws concerning animal experiments.

The animals were injected intramuscularly in the left thigh, after being anesthetized with a mixture of medetomide (Dormitor; Pfizer), ketamine hydrochloride (Ketalar; Warner-Lambert), and saline (1:1:8), with 100 μL of *E. coli* (2×10^8 cfu/mL), 100 μL of *S. aureus* (2×10^8 cfu/mL), 100 μL of *C. albicans* (2×10^8 cfu/mL), or 100 μL of *A. fumigatus* (1×10^8 cfu/mL) 24 h before injection of ^{123}I-chitinase. Sterile inflammation was induced by injecting 50 μL of terpentine (Sigma-Aldrich) 24 h before injection.

Postmortem Microorganism Cultivation

To verify whether the respective injected species were still apparent in the induced infections postmortem, cultures were grown.

The left thigh was aseptically removed from the mice and mixed in 2 mL of PBS using a tissue homogenizer for 45 s at 9,000 rpm. Serial 10-fold dilutions were spread onto the respective testing plates and incubated as described, after which cfu were counted. As a control, tissue of uninfected and sterile inflamed thigh muscle was similarly examined.

Biodistribution

The tracer was injected in NMRI mice intravenously through the lateral tail vein with 100 μL (±37 kBq) of ^{123}I-ChiB_E144Q. During the experiments, animals obtained food and water ad libitum. At 20 and 40 s, 1, 1.5, 2, 3, 5, 10, 20, 30, and 40 min, and 1, 2, 3, 6, 9, 15, 24, and 48 h after injection, the animals were anesthetized and killed by decapitation ($n = 3$). Blood samples and tissue samples of lung, liver, stomach, spleen, bladder, large intestine, small intestine, brain, heart, and fatty tissue were dissected, weighed, and counted for radioactivity with a multichannel NaI detector (Cobra Packard). To calculate uptake of the tracer in each tissue sample as a percentage of the injected dose (%ID), aliquots of the injected dose were weighed and counted simultaneously. The concentration of radioactivity was expressed as %ID per gram of tissue (%ID/g).

Scintigraphy

The in vivo imaging characteristics of ^{123}I-ChiB_E144Q were studied in Swiss *nu/nu* mice with intramuscular infections of *C. albicans*, *A. fumigatus*, *E. coli*, or *S. aureus* and sterile inflammation in the left thigh muscle by planar scintigraphy. During the experiments animals obtained food and water ad libitum.

Planar scintigraphic images were acquired at 5 and 24 h after injection of the tracer by placing the animals in a ventral position on a planar γ-camera (GCA-9300A/hg; Toshiba), equipped with low-energy, high-resolution, parallel-hole collimators. The energy window used was 159 keV ± 20%. Images (±350,000 counts) were stored in a 1,024 × 1,024 matrix and processed with a Hermes image process system. The animals were anesthetized as described 5 min before scanning.

After scanning, at 24 h after injection of the radiolabeled chitinase, the mice were killed with 10 mg of phenobarbital injected intraperitoneally. Blood was obtained by cardiac puncture. Tissue samples of right muscle, infected left muscle, lung, spleen, kidney, liver, and intestine were dissected and weighed, and their activity was measured in a multichannel NaI detector (Cobra Packard). To calculate uptake of the radiolabel in each tissue sample as a fraction of the injected dose, aliquots of the injected dose were counted simultaneously. The results are expressed as %ID/g. Abscess-to-blood and abscess-to-muscle ratios were calculated.

Statistical Analysis

Differences between in vitro binding study results and biodistribution or accumulation of infected thigh muscle caused by the various microorganisms were evaluated with the Student *t* test. All results are given as mean ± SEM.

RESULTS

Radiolabeling and Characterization of ^{123}I-ChiB_E144Q

The yield of the labeling reaction at various reaction times is shown in Table 1. On average, a radiochemical yield of 35% was obtained. Radiochemical purity was >97% with a stability of >24 h in PBS as determined by ITLC. After a 30-h incubation in murine serum, a loss of 20% of radiolabel was seen (Fig. 1). The radiochemical purity was additionally determined quantitatively by HPLC, by measuring the injected amount of radioactivity and the retained and collected radioactivity after 1 run. Free iodine remains at the beginning of the column. The ultraviolet

TABLE 1
Various Reaction Times and Corresponding Labeling Efficiency of ^{123}I-ChiB_E144Q

Reaction time (min)	Radiochemical yield (%)
5	10.81
10	34.87
10	41.64
10	34.95
20	44.49
30	40.31

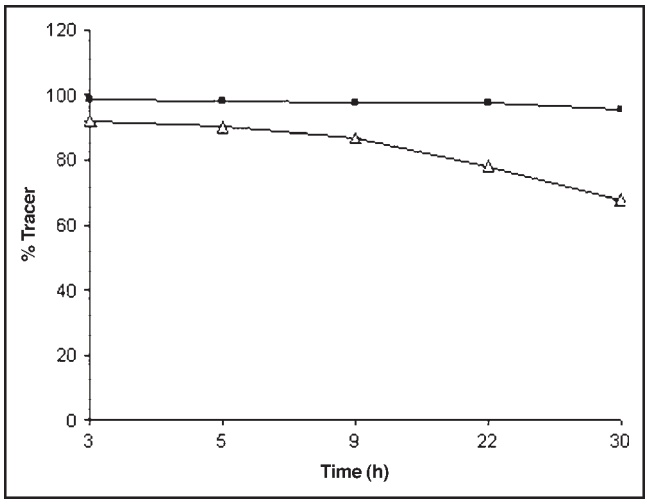

FIGURE 1. Stability of ^{123}I-ChiB_E144Q in PBS as determined by ITLC ($n = 5$). △, in serum; ■, in PBS.

(UV) profile and radiochromatogram, as determined by HPLC, showed 1 peak each with similar retention times of 6.13 ± 0.48 min (Fig. 2). No significant side peaks were detected. The average specific activity of the ^{123}I-chitinase was 168.2 MBq/mol (9.25 MBq/μg) protein.

In Vitro Binding Studies

The amount of radioactivity bound to various types of cells, after overnight incubation, 1 washing step, and correction for nonspecific binding varied from virtual no binding to *S. aureus* and *E. coli* to a maximum of 2.4×10^3 Bq per 1×10^7 cells for *A. fumigatus* and 3.0×10^3 Bq per 1×10^7 for *C. albicans* ($P < 0.05$). Studies with various amounts of tracer added showed clear dose–response relationships for binding to *A. fumigatus* and *C. albicans* (Fig. 3). No significant binding was observed if the target organisms were preincubated with a 50-fold excess of unlabeled ChiB_E144Q.

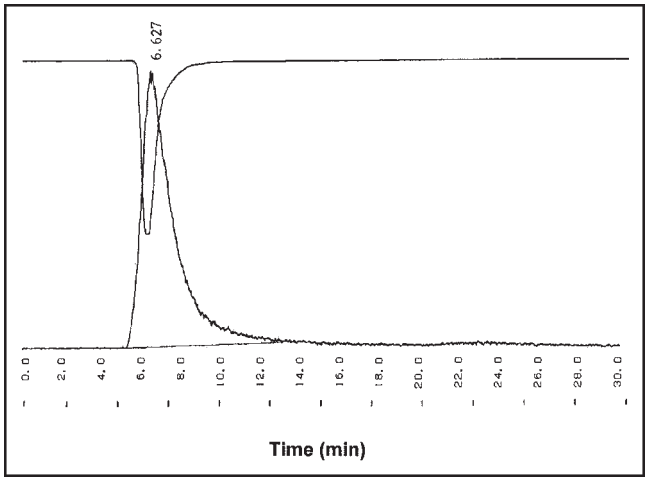

FIGURE 2. Typical UV profile (280 nm) of unlabeled ChiB_E144Q (upside down) combined with radiogram of ^{123}I-ChiB_E144Q.

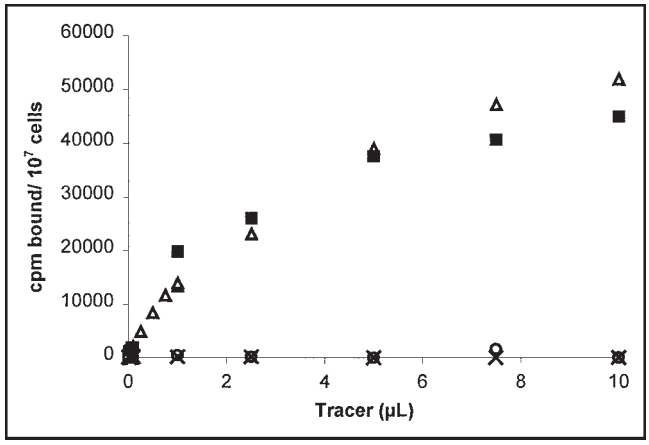

FIGURE 3. In vitro accumulation of ^{123}I-ChiB_E144Q in various organisms after 24-h incubation at 4°C. Amount of tracer bound per 1×10^7 cfu is plotted as function of increasing amounts of added tracer (1 μL = 2×10^3 Bq). ■, *C. albicans*; ○, *E. coli*; △, *A. fumigatus*; ×, *S. aureus*.

Binding to Mammalian Cells

The radioligand showed no or little accumulation in the separated erythrocyte and leukocyte fractions. After centrifugation of the coagulated protein fraction, the pellet accounted for >50% of the total activity in the blood sample. To correct for the respective amounts of the different fractions, results are expressed in %activity/% (g) blood (Table 2). To ensure that free ^{123}I was not enclosed in the protein pellet, additional control experiments were performed in a similar setup, showing a different distribution between the various cell types, protein fraction, and remaining supernatant. Free ^{123}I appears to accumulate more in erythrocytes and leukocytes, and its presence in the final supernatant is >10 times higher in comparison with the tracer. Most of the tracer is found in the protein fraction, indicating that a considerable amount of the circulating tracer is still intact at 24 h after injection

Biodistribution

The results obtained from the biodistribution in noninfected NMRI mice (Table 3) showed that the compound almost fully cleared from the blood pool at 48 h after injection (Fig. 4). The stomach and bladder had the highest

TABLE 2
Binding of ^{123}I-ChiB_E144Q to Mammalian Cells In Vivo at Different Time Points

Fraction	1 h	4 h	8 h	18 h	24 h	24 h*
Erythrocyte	0.14	0.10	0.09	0.09	0.07	0.35
Leucocyte	0.02	0.04	0.02	0.07	0.02	0.45
Protein	2.82	2.19	3.35	3.91	3.20	1.12
Free ^{123}I	0.04	0.06	0.05	0.06	0.05	0.65

*Distribution data at 24 h after injection of free ^{123}I as control. Data are expressed as % activity/% (g) blood.

TABLE 3
Biodistribution Results of ^{123}I-ChiB_E144Q in Noninfected NMRI Mice

Biodistribution	20 min	1 h	4 h	9 h	24 h	48 h
Blood	14.23 ± 3.80	13.37 ± 1.01	5.09 ± 1.54	3.62 ± 0.43	0.83 ± 0.11	0.20 ± 0.03
Brain	0.29 ± 0.12	0.30 ± 0.08	0.18 ± 0.15	0.11 ± 0.02	0.03 ± 0.03	0.03 ± 0.04
Heart	3.80 ± 1.43	4.89 ± 1.85	1.40 ± 0.53	1.17 ± 0.40	0.35 ± 0.06	0.18 ± 0.13
Lung	5.01 ± 3.59	5.86 ± 1.40	1.86 ± 0.70	0.92 ± 1.17	0.42 ± 0.11	0.14 ± 0.04
Stomach	1.96 ± 1.30	4.89 ± 3.13	8.78 ± 4.10	6.64 ± 6.67	0.55 ± 0.12	0.11 ± 0.12
Spleen	3.69 ± 0.55	3.18 ± 0.23	1.23 ± 0.51	0.95 ± 0.05	0.22 ± 0.03	0.09 ± 0.06
Liver	2.32 ± 0.43	1.92 ± 0.90	0.99 ± 0.36	0.66 ± 0.12	0.19 ± 0.01	0.07 ± 0.01
Kidneys	5.23 ± 1.85	5.20 ± 0.93	2.18 ± 0.55	1.39 ± 0.27	0.45 ± 0.28	0.18 ± 0.09
Small intestine	0.72 ± 0.20	1.54 ± 0.11	1.00 ± 0.21	0.50 ± 0.57	0.14 ± 0.01	0.04 ± 0.02
Large intestine	0.52 ± 0.20	0.79 ± 0.21	0.88 ± 0.04	0.65 ± 0.71	0.11 ± 0.05	0.05 ± 0.01
Bladder	6.40 ± 4.40	1.62 ± 0.38	2.93 ± 2.01	1.57 ± 1.14	0.44 ± 0.33	0.44 ± 0.31
Fatty tissue	1.55 ± 0.53	1.19 ± 1.12	1.16 ± 0.89	0.53 ± 0.22	0.22 ± 0.06	0.10 ± 0.03

Data are expressed as %ID/g ± SD (n = 3 mice/group). Represented data are a selection from 19 different time points ranging from 20 s to 48 h.

retention of radiolabel at later time points (>20 h). Accurate dissection of the thyroid made it difficult to obtain reproducible accumulation results and varied from 1.49 to 3.99 %ID/g at 24 h after injection

Scintigraphy Results

Images 5 h after injection of the tracer showed little uptake in both bacterial and fungal infectious foci (data not shown), whereas images at 24 h after injection (Fig. 5) showed uptake in fungus-infected thigh muscles only. Scintigraphy was in accordance with the data of postmortem activity counting and showed high accumulation in the stomach, thyroid, and bladder.

Directly after scintigraphy at 24 h after injection, the animals were killed and dissected, tissue samples were weighed, and the activity was measured. Except for the bladder, thyroid, and stomach, the highest uptake of ^{123}I-ChiB_E144Q was found in the abscess of fungus-infected mice (Table 4). Target-to-nontarget (T/NT) ratios, as calculated from the biodistribution data postmortem, were 20.6 ± 3.6 for *C. albicans* and 15.2 ± 3.7 for *A. fumigatus* infections, respectively, whereas T/NT ratios for *S. aureus*– and *E. coli*–infected thigh muscles did not exceed 4.9 ± 2.6 and 3.0 ± 2.3, respectively. In mice

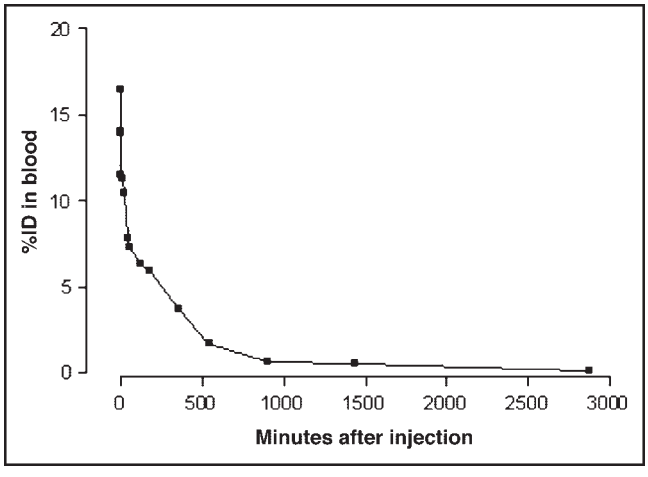

FIGURE 4. In vivo blood clearance (%ID) in healthy NMRI mice until 48 h after injection. Half-life ($t_{1/2}$) parameters are calculated. Blood clearance follows a biexponential curve with equation (r^2 = 0.987): $A = A_1 \exp(-\lambda_1 t) + A_2 \exp(-\lambda_2 t)$ with $t_{1/2,1}$ = 0.144 ± 0.035, $t_{1/2,2}$ = 4.229 ± 0.701 and A_1 = 6.436 ± 0.700 (%ID) and A_2 = 9.053 ± 0.661 (%ID), λ_1 = 0.1011 ± 0.0309 (min^{-1}), λ_2 = 0.0027 ± 0.0309 (min^{-1}).

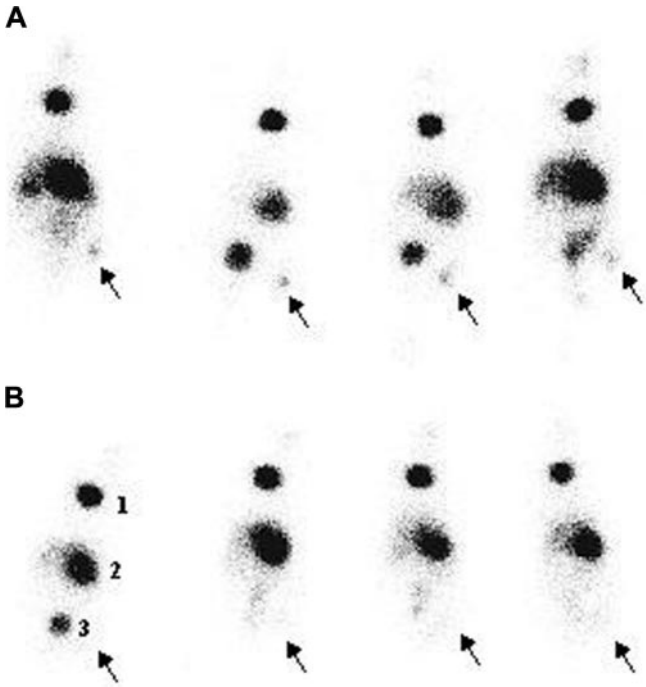

FIGURE 5. Scintigraphic images of *nu/nu* mice (n = 4) with unilateral infections of 1 × 10^7 conidia of *A. candida* (A) and 1 × 10^7 cfu of *S. aureus* (B) 24 h after injection of 7.4 MBq in 100 μL of ^{123}I-ChiB_E144Q. Arrows indicate site of infection. 1 = thyroid; 2 = stomach; 3 = bladder.

TABLE 4
Biodistribution Data of ^{123}I-ChiB_E144Q in Infected *nu/nu* Mice 24 h After Injection

Biodistribution	*C. albicans*	*A. fumigatus*	*E. coli*	*S. aureus*	Sterile inflammation	*A. fumigatus**
Blood	0.70 ± 0.02	0.66 ± 0.05	0.92 ± 0.59	0.72 ± 0.13	0.66 ± 0.05	0.99 ± 0.31
Muscle	0.09 ± 0.01	0.11 ± 0.08	0.24 ± 0.16	0.10 ± 0.02	0.11 ± 0.08	0.27 ± 0.10
Abscess	1.91 ± 0.13	2.07 ± 0.01	0.47 ± 0.31	0.46 ± 0.26	0.60 ± 0.06	0.47 ± 0.19
Lung	0.37 ± 0.09	0.31 ± 0.02	0.42 ± 0.14	0.45 ± 0.04	0.47 ± 0.02	0.87 ± 0.07
Spleen	0.26 ± 0.03	0.18 ± 0.02	0.24 ± 0.03	0.31 ± 0.05	0.16 ± 0.02	6.37 ± 1.29
Kidney	0.61 ± 0.13	0.29 ± 0.04	0.41 ± 0.10	0.52 ± 0.10	0.26 ± 0.05	3.28 ± 1.08
Liver	0.35 ± 0.01	0.22 ± 0.02	0.23 ± 0.04	0.38 ± 0.05	0.16 ± 0.02	16.32 ± 3.83
Intestine	0.27 ± 0.04	0.07 ± 0.02	0.21 ± 0.09	0.23 ± 0.03	0.08 ± 0.02	0.41 ± 0.11
Bladder	1.60 ± 0.58	0.73 ± 0.33	0.57 ± 0.27	0.62 ± 0.27	0.41 ± 0.32	1.29 ± 0.32
Stomach	3.06 ± 1.57	0.82 ± 0.25	3.48 ± 2.55	2.47 ± 0.48	0.74 ± 0.25	2.16 ± 1.38

*Results of ^{123}I-BSA in *A. fumigatus* infection.
Data are expressed as %ID/g ± SD (n = 4 mice/group).

with induced sterile inflammation, T/NT ratios were 5.3 ± 2.8. The %ID/g of fungus-infected thighs was always higher than that in thighs infected with bacteria or with induced sterile inflammation ($P < 0.05$). The T/NT ratio of radiolabeled BSA in *C. albicans* infections was 2.11 ± 0.57 (Table 5). Target-to-blood ratios for fungus-infected thighs were always >1.

The uptake of the tracer in *C. albicans* and *E. coli* infections was followed in time. Until 6 h after injection of the tracer, no significant difference was seen between the T/NT ratios of both types of infection, as calculated from biodistribution data postmortem. At this point, scintigraphic images showed equal intensities at sites of infection for both types of infection (results not shown). From then on, the T/NT ratio of ^{123}I-ChiB_E144Q in *C. albicans* infections increased to a significant extent (Fig. 6).

In an additional experiment, the uptake of tracer correlated with the amount of viable cfu of *C. albicans* previously injected in thigh muscle tissue is shown in Figure 7.

TABLE 5
Comparison of T/NT and Target-to-Blood Ratios as Calculated from Biodistribution Data of Different Radioligands in Infected *nu/nu* Mice 24 h After Injection

Infection	^{123}I-ChiB_E144Q	^{123}I-BSA	^{67}Ga Citrate
C. albicans			
Muscle	20.62 ± 3.06	2.11 ± 0.57	4.83 ± 0.48
Blood	2.72 ± 0.25	0.59 ± 0.11	1.57 ± 0.07
A. fumigatus			
Muscle	15.16 ± 3.72	1.44 ± 1.69	5.59 ± 2.72
Blood	1.47 ± 0.22	0.60 ± 0.79	3.06 ± 1.26
E. coli			
Muscle	3.03 ± 2.30	1.69 ± 0.89	3.11 ± 1.28
Blood	0.57 ± 0.40	0.34 ± 0.14	1.43 ± 0.49
S. aureus			
Muscle	4.86 ± 2.62	ND	ND
Blood	0.62 ± 0.24	ND	ND
Sterile inflam.			
Muscle	5.31 ± 2.83	ND	ND
Blood	0.91 ± 0.81	ND	ND

ND = not determined; inflam. inflammation.
Data are expressed as %ID/g ± SD (n = 4 mice/group).

Postmortem Microorganism Cultivation

Twenty-four hours after inoculation, the infected thigh muscles were slightly swollen. Dissection of the infectious site revealed localized microorganisms in the examined muscle tissue and slight pus formation. Postmortem counting of viable bacteria, fungi, and yeast cells in infected tissue samples was always positive. Values were generally >10^6 cfu/g tissue for all organisms, respectively. Aseptically removed tissue of uninfected and sterile inflamed thigh muscle resulted in negligible viable counts of the various organisms.

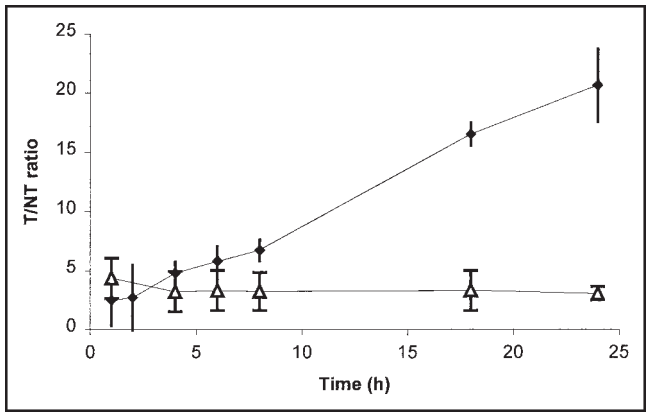

FIGURE 6. Uptake expressed as T/NT ratio ± SD (n = 3) of ^{123}I-ChiB_E144Q in *E. coli* infections (△) and *C. albicans* infections (◆) until 24 h after infection.

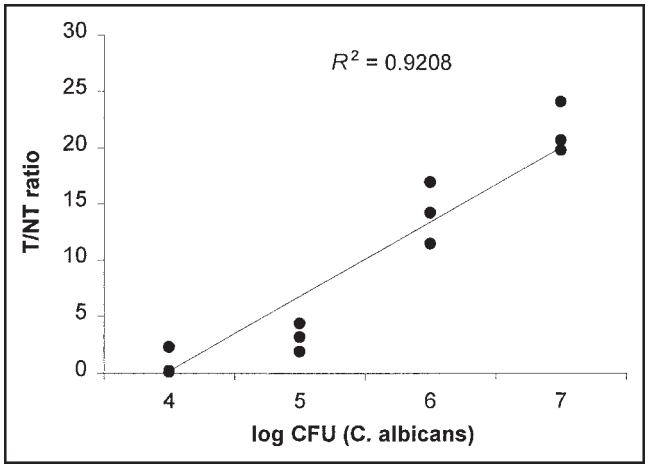

FIGURE 7. Relation between number of injected viable *C. albicans* and accumulation of ^{123}I-ChiB_E144Q, expressed as T/NT ratio in infected tissue in Swiss *nu/nu* mice ($n = 3$).

DISCUSSION

This study shows that ChiB_E144Q can be labeled with ^{123}I with a moderate radiochemical yield and high stability. Different reaction times did not improve the radiochemical yield significantly. The labeled ChiB_E144Q showed specific binding to chitin-containing *C. albicans* and *A. fumigatus*. After adding a 50-fold excess of unlabeled ChiB_E144Q, the amount of activity bound to 1×10^7 cfu dropped to zero. The labeled chitinase did not interact, or barely interacted, with gram-positive or gram-negative bacteria (in vitro and in vivo), presumably due to the absence of chitin in the bacterial cell wall. These results indicate specific binding of the labeled ChiB_E144Q to fungi.

The activity bound to 1×10^7 cfu of *C. albicans* in vitro was significantly higher than that for *A. fumigatus*, at least for the highest amounts of tracer added. This is probably due to differences in the percentage of chitin between both fungal cell walls or to differences in the accessibility of the chitin to the enzyme.

On the basis of the in vitro results, we examined the potential of ^{123}I-ChiB_E144Q as a fungus-specific tracer in vivo in mice with infected thigh muscles. The abscess uptake of ^{123}I-ChiB_E144Q in fungal infections was $>10\times$ higher than the uptake of ^{123}I-BSA in identical infections and $>3\times$ higher than the uptake in bacterial infections. A similar low accumulation was found in thigh muscles with sterile inflammation. Together these results clearly show that abscess uptake is a result of a specific interaction between the labeled chitinase and fungi, presumably via the chitin in their cell walls. These findings are confirmed by a good correlation ($R^2 = 0.924$, $P < 0.05$) between the T/NT ratios for the tracer and the number of injected viable *C. albicans*.

The results showed high uptake of ^{123}I in the thyroid and stomach. Previous studies have shown that radioiodinated peptides are rapidly dehalogenated in vivo, which is reflected in high radioiodine levels in the thyroid and stomach (*21,22*). High values of activity in the liver and spleen are often seen in biodistribution data of radiolabeled proteins. Therefore, proteins such as ChiB_E144Q, with a molecular weight ~60 kDa, are not retained in the kidneys (*23,24*).

The use of chitinase as a tracer implies that a wide variety of proteins from the glycosyl hydrolase families 18 and 19, derived from all kinds of different species, could be examined for their functionality in this respect. By reducing the size of these proteins, fragments such as the small chitin-binding domain might show interesting characteristics for in vivo imaging, resulting in rapid uptake, fast blood clearance, and, thus, faster visualization (*25*).

Specific imaging of fungal infections with radiopharmaceuticals has been investigated in the past. Becker et al. (*8*) examined the potential of ^{99m}Tc-PEG–liposomes for the detection of experimental invasive pulmonary aspergillosis (IPA) in neutropenic rats. The preparation was found to diagnose IPA as early as 48 h after injection of the respective tracer with an infected-to-noninfected lung ratio ranging from 2.67 at 48 h to 5.91 at 168 h. Although not designed to interact specifically with *A. fumigatus* itself, ^{99m}Tc-PEG–liposomes were able to detect IPA twice as fast as other existing techniques, such as monitoring galactomannan levels in serum. This result stresses the simplicity and accuracy of radiopharmaceuticals for diagnosis of IPA. Welling et al. (*26*) performed studies with ^{99m}Tc-labeled antimicrobial peptides to detect bacterial and *C. albicans* infections in vivo. ^{99m}Tc-Antimicrobial peptides accumulated in a significantly higher rate in bacterial and *C. albicans* infections than that in inflamed tissues in thigh muscles of mice and rabbits as early as 1 h after injection, suggesting that the preparation could differentiate infection from inflammation but could not make the distinction between bacterial or fungal infection. ^{99m}Tc-Labeled fluconazole was developed by Lupetti et al. to examine the compound's ability to specifically detect *C. albicans* and *A. fumigatus* infections in mice (*6*). One hour after injection, ^{99m}Tc-fluconazole could only detect *C. albicans* infections in vivo. Accumulation in bacterial infections, *A. fumigatus* infections, and sterile inflammation remained significantly lower.

^{123}I-ChiB_E144Q yielded fair T/NT ratios (15.16–20.6), specific accumulation at sites infected with *C. albicans* as well as *A. fumigatus*, and low uptake in bacterial infection or sterile inflammation. Due to the molecular size of ChiB_E144Q, the blood clearance is slower than that of the smaller tracers mentioned. Although all infections could be detected from early time points onward, distinction between fungal and bacterial infections was possible at later time points with a maximum at 24 h after injection.

The use of ^{123}I-ChiB_E144Q as a specific tracer for fungal infection has some drawbacks. Currently, the compound is not readily available since commercial production has not yet been established. Furthermore, possible toxicologic and immunologic effects must be examined.

CONCLUSION

This study is a new step toward the specific imaging of fungal infections. It shows that ^{123}I-ChiB_E144Q can be used as a tracer for imaging fungal infection. The ability of this radioiodinated enzyme to accumulate in both *C. albicans* and *A. fumigatus* infectious lesions and the good correlation found between the T/NT ratio and the number of viable *C. albicans* highlight the specificity of its binding. Accumulation of ^{123}I-ChiB_E144Q was considerably lower in sterile inflammations or bacterial infections in Swiss *nu/nu* mice ($P < 0.05$). Of course, possible undesirable effects of ^{123}I-ChiB_E144Q must be examined, although no toxicologic or immunologic side effects were observed during the in vivo experiments.

Future experiments will include the labeling of ^{99m}Tc to a hydrazinonicotinamide conjugate of ChiB_E144Q, which is not expected to show any thyroid and stomach uptake, which is quite disturbing for scintigraphic imaging. Furthermore, other fungal infections will be examined in a similar setup or in more clinical models, such as invasive pulmonary aspergillosis.

ACKNOWLEDGMENTS

The authors thank Bjornar Synstad and Xiaohong Jia (Department of Chemistry and Biotechnology, Agricultural University of Norway) for help in preparing ChiB_E144Q. This research was supported in part by an award from the International Society of Radiolabeled Blood Elements.

REFERENCES

1. Boerman O, Rennen H, Oyen WJ, Corstens FH. New concepts in infection/inflammation imaging. *Q J Nucl Med.* 2001;45:167–173.
2. de Winter F, Vogelaers D, Gemmel F, Siaens R, Slegers G, Dierckx R. The rising incidence of invasive fungal infections: is there a role for nuclear medicine? In: Hossri Nogueira Braga FJ, ed. *Nuclear Medicine in Tropical Infectious Diseases.* Boston, MA: Kluwer Academic; 2002:200–208.
3. Kontoyiannis DP, Bodey GP. Invasive aspergillosis in 2002: an update. *Eur J Clin Microbiol Infect Dis.* 2001;21:161–172.
4. Denning DW. Invasive aspergillosis. *Clin Infect Dis.* 1998;26:781–805.
5. Frazier DD, Cambell DR, Garvey TA, Wiesel SA, Bolhman HH, Eismont FJ. Fungal infections of the spine. *J Bone Joint Surg Am.* 2001;83:560–565.
6. Lupetti A, Welling MM, Mazz U, Nibbering PH, Pauwels EKJ. Technetium-99m labelled fluconazole and antimicrobial peptides for imaging of *Candida albicans* and *Aspergillus fumigatus* infections. *Eur J Nucl Med.* 2002;29:674–679.
7. Stynen D, Sarfati J, Goris A, et al. Rat monoclonal antibodies against Aspergillus gallactomannan. *Infect Immun.* 1992;60:2237–2245.
8. Becker MJ, Dams ET, de Marie S, et al. Scintigraphic imaging using ^{99m}Tc-labeled PEG liposomes allows early detection of experimental invasive pulmonary aspergillosis in neurtopenic rats. *Nucl Med Biol.* 2002;29:177–184.
9. Rubin RH, Fischman AJ. Radionuclide imaging of infection in the immunocompromised host. *Clin Infect Dis.* 1996;22:414–423.
10. Wills EA, Redinbo MR, Perfect JR, Poeta MD. New potential targets for antifungal development. *Expert Opin Ther Targets.* 2002;4:265–296.
11. Koga D, Mitsutomi M, Kono M, Matsumiya M. Biochemistry of chitinases. In: Jollès P, Muzzarelli RA, eds. *Chitin and Chitinases.* Berlin, Germany: Birkhäuser Verlag; 1999:111–123.
12. Renkma GH, Boot RG, Muijsers AO, Donker-Koopman WE, Aerts JM. Purification and characterization of human chitotriosidase, a novel member of the chitinase family of proteins. *J Biol Chem.* 1995;270:2198–2202.
13. Tjoelker LW, Gosting L, Frey S, et al. Structural and functional definition of the human chitinase chitin-binding domain. *J Biol Chem.* 2000;275:514–520.
14. Robertus JD, Monzingo AF. The structure and action of chitinases. In: Jollès P, Muzzarelli RA, eds. *Chitin and Chitinases.* Berlin, Germany: Birkhäuser Verlag; 1999:125–135.
15. van Aalten DMF, Synstad B, Bruberg MB, et al. Structure of a two-domain chitotriosidase from Serratia marcescens at 1.9-Å resolution. *Proc Natl Acad Sci USA.* 2000;97:5842–5847.
16. Synstad B, Gåseidnes S, Vriend G, Nielsen J-E, Eijsink VGH. On the contribution of conserved acidic residues to catalytic activity of chitinase B from *Serratia marcescens*. In: Peter MG, Muzzarelli RAA, Domard A, eds. *Advances in Chitin Science.* Vol. 4. Ås, Norway: University of Norway; 2000:524–529.
17. Watanabe T, Ariga Y, Sato U, et al. Aromatic residues within the substrate-binding cleft of Bacillus circulans chitinase A1 are essential for crystalline chitin hydrolysis. *Biochem J.* 2003;376:237–244.
18. Watanabe T, Ishibashi A, Ariga Y, et al. Trp122 and Trp134 on the surface of the catalytic domain are essential for crystalline chitin hydrolysis by Bacillus circulans chitinase A1. *FEBS Lett.* 2001;494:74–88.
19. Uchiyama T, Katouno F, Nikaidou N, Nonaka T, Sugiyama J, Watanabe T. Roles of the exposed aromatic residues in crystalline chitin hydrolysis by chitinase A from Serratia marcescens 2170. *J Biol Chem.* 2001;276:41343–41349.
20. Brurberg MB, Nes IF, Eijsink VGH. Comparative studies of chitinases A and B from Serratia marcescens. *Microbiology.* 1996;142:1581–1589.
21. Garg PK, Alston KL, Welsh PC, Zalutsky PR. Enhanced binding and inertness to dehalogenation of melantropic peptides labelled using N-succinimidyl 3-iodobenzoate. *Bioconjug Chem.* 1996;7:233–239.
22. Larsen RH, Murud KM, Akabani G, Hoff P, Bruland OS, Zalutsky MR. ^{221}At- and ^{131}I-labeled biphosphonates with high in vivo stability and bone accumulation. *J Nucl Med.* 1999;40:1197–1203.
23. Sumpio BE, Maack T. Kinetics, competition and selectivity of tubular absorption of proteins. *Am J Physiol.* 1982;243:F379–F392.
24. Behr TM, Goldenberg DM, Becker W. Reducing the renal uptake of radiolabeled antibody fragments and peptides for diagnosis and therapy: present status, future prospects and limitations. *Eur J Nucl Med.* 1998;25:201–212.
25. van Aalten DM, Komander D, Synstad B, Gaseidne S, Peter MG, Eijsink VGH. Structural insights into the catalytic mechanism of a family 18 exo-chitinase. *Proc Natl Acad Sci USA.* 2001;98:8979–8984.
26. Pauwels EKJ, Welling MM, Nibbering PH, Lupetti A, Balter HS. ^{99m}Tc-Labeled antimicrobial peptides for detection of bacterial and *Candida albicans* infections [reply to letter]. *J Nucl Med.* 2002;43:1126–1127.